

# Postcollisional evolution features of the intracontinental structures formed by overthrusting

O.I. Parphenuk

Schmidt Institute of Physics of the Earth of the Russian Academy of Sciences, Moscow, Russian Federation

E-mail: [oparfenuk@ifz.ru](mailto:oparfenuk@ifz.ru)

**Abstract.** The investigation of intracontinental collision structures is conducted based on the complex model of the thermal and mechanical evolution of overthrusting process for the rheologically layered lithosphere, which includes brittle upper crust, the lower crust and lithospheric upper mantle with different effective viscosity values. Finite element models with Lagrangian approach were used for the problem simulation. It was shown that thermal evolution of continental orogens essentially results from the geometry and topography due to thrusting and postcollision stage. This work concentrates on the thermal parameters influence on the evolution of collision zones aimed to the study of possibility of granite melt formation. Calculations for mean continental initial temperature distribution lead to the conclusion of possibility of granite melt formation for the case of “wet” granite solidus. The horizon of temperatures higher than “wet” granite solidus appears at the level of 30-40 km, moving upward to the depth 15-20 km at postcollision stage. The early postcollision evolution shows some heat flow increase due to the thickening of the upper crust with maximum heat generation rate. Further history leads to the stable heat flow values because additional loading redistribution resulting from the denudation of surface uplift and corresponding sedimentation is small due to the local erosion in our model. It was shown that surface heat losses after the termination of horizontal shortening depend to a greater extent on radiogenic heat generation rather than thermal conductivity value in the upper crust.

**Keywords:** collision, overthrusting, evolution, heat generation, heat flow value, thermal conductivity, rheology, temperature, solidus

**Recommended citation:** Parphenuk O.I. (2018). Postcollisional evolution features of the intracontinental structures formed by overthrusting. *Georesursy = Georesources*, 20(4), Part 2, pp. 377-385. DOI: <https://doi.org/10.18599/grs.2018.4.377-385>

It is known that vast areas of deeply eroded folded areas of the Earth, for example, ancient shields, are composed mainly (by 70-80%) of granitoids associated with the processes of partial melting and metamorphism in the crust thickened during a collision. Granite-gneiss allochthonous, indicating the tectonic stratification of the continental crust, are described in the Himalayas, the Pamirs, the Caledonides of Norway, Sweden and many other areas (Sokolov, 1999). One of the distinguishing features of the collision areas is the formation of granite melts under partial melting conditions, and in some cases the appearance of a granite layer on the surface as a result of erosion of the mountain uplift. The Early Proterozoic accretion of granite-greenstone and granulite-gneiss terranes joined by collision zones led to the formation of the Siberian craton. On the modern surface of the erosion slice, the collision zones of terranes reflect the level of the middle and lower crust brought to the surface and eroded

at the postcollisional stage when the upper crust, including granitoids, which were melted and intruded into the upper crust, was completely eroded (Rosen, Fedorovskii, 2001).

Early Paleozoic collision systems make it possible to see the granite layer, which appeared at the surface due to the erosion of the mountain uplift and formed the upper crust with a thickness of about 10 km (European variscides). This layer could result from warming up inside the thickened crust during or after the termination of the collision (Gerdes et al., 2000).

## Lapland granulite belt – an example of the early Proterozoic collision orogen

The Baltic shield is the largest projection of the ancient crystalline basement of the East European Platform and is favorable for studying the internal structure of the crystalline crust, since there is no distorting effect of the sedimentary cover. Within the framework of the EGT (European Geotraverse) project, a 500-km POLAR profile was obtained by the method of reflected seismic waves, passing to the north of the Baltic (Fennoscandinavian) shield through several Archean

and Early Proterozoic crustal segments. Figure 1 shows the main tectonic elements of the region with a length of 100×500 km along the POLAR profile: the Lapland part of the Karelian province, the Archean Terranes of Inari and Servaranger, the Early Proterozoic Lapland granulite and Polmak-Pasvik-Pechenga belts. According to modern data, the Lapland granulite belt is a complexly constructed body, pulled in a southwesterly direction to the Karelian province (the northern part of the Karasjok – Kittila greenstone belt) at an angle of 30° (Gaal et al., 1989, Sharov, 1993). Between these tectonic structures there is a relatively narrow tectonic zone – the Tanaelv belt (Tana), bordering the southern and western contacts of the Lapland granulite belt (Perchuk et al., 1999).

Figure 2 gives an idea of the metamorphic zonation along the POLAR profile area and confirms the general tendency of increasing the degree of metamorphism in the direction of thrust and the maximum P-T conditions of metamorphism in the zone of the limiting fault. When crossing the Lapland granulitic belt in the direction of thrust, the equilibrium temperatures increase from 750 to 820°C, and pressures from 6.5 to 7 kbar, showing the metamorphism of higher stages (Gaal et al., 1989).

The rocks of the Lapland granulite belt of the Baltic Shield were pulled in a southwesterly direction to the underlying rocks of the Karelian province, forming the

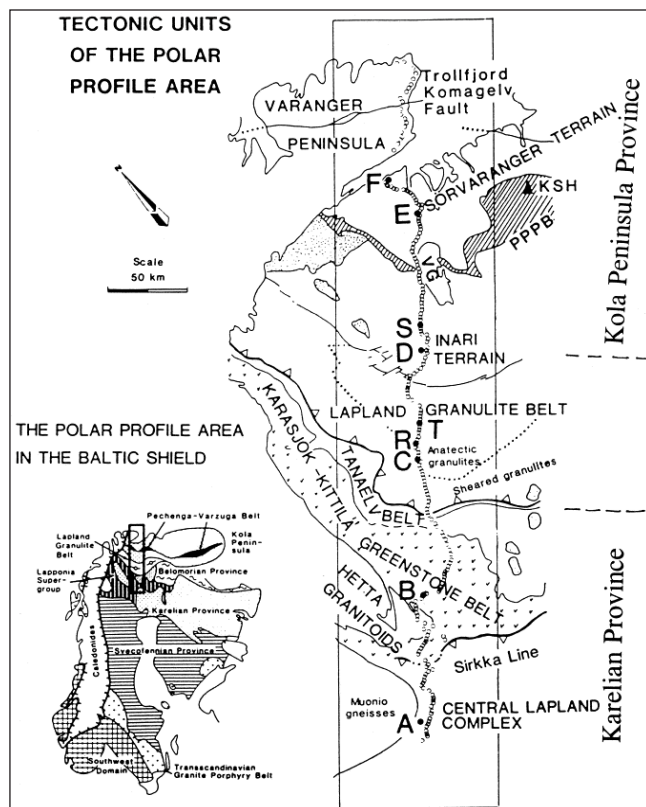


Fig. 1. Tectonic units of the POLAR profile location area (Gaal et al., 1989). Capital Latin letters indicate points of explosions, circles indicate the position of seismographs. PPPB – Polmak-Pasvik-Pechenga belt. SG-3 – the location of the Kola ultradeep well

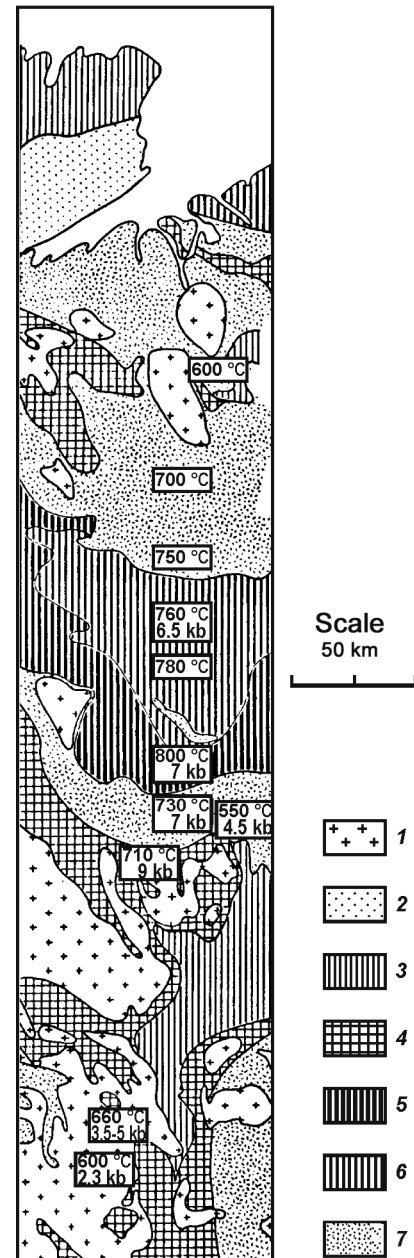


Fig. 2. Metamorphic zonation of the POLAR profile region: 1 – igneous rocks; 2 – very low level; 3 – low level; 4 – medium level; 5 – granulitic facies; 6 – granulitic facies with cordierite; 7 – high stage, migmatites. The numbers in the figure show the P-T estimates of the metamorphism conditions. The position of the region corresponds to Fig. 1 (Tectonophysics, 1989)

tectonic zone of the Tanaelv belt (Tectonophysics, 1989; Barbey et al., 1984). Figure 3 shows a diagram of the crust structure and the isolines of seismic waves velocity. The high-velocity body with seismic velocities of 6.3 to 6.6 km/s in the upper part of the model was created by the Lapland granulite belt, the Tanaelv and Karasjok-Kittila belts. Due to the more extended nature of the thrust, as mentioned above, the anomaly is also more stretched in the horizontal direction and complicated by the processes apparently imposed later. Under the Lapland belt itself, the Moho depth is less than that to

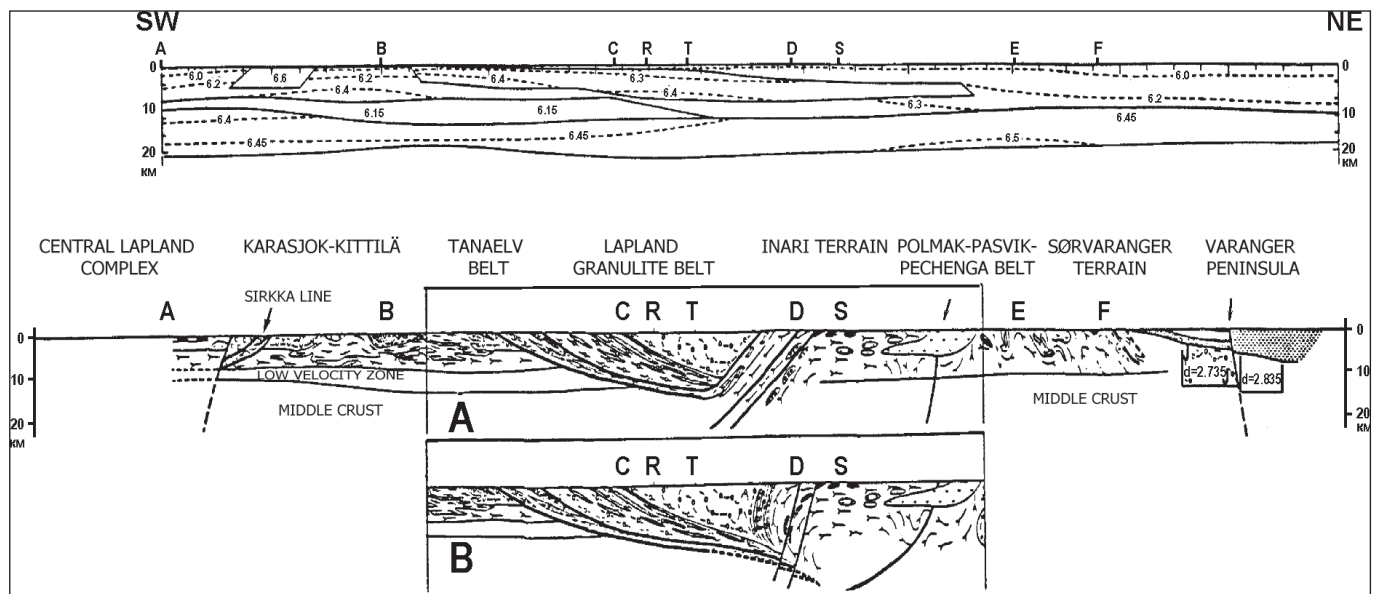


Fig. 3. The upper 20 km of the seismic model and the geological section along the POLAR profile (Gaal et al., 1989). The corresponding designations are shown in Fig. 1

the south and is approximately 40 km with a maximum value of 47 km (Luosto et al., 1989).

This is an example of an ancient intra-collisional structure, in the modern structure of which there is no Moho depression with an increase in the crust thickness in the process of thrusting. There are examples of compressional orogens that have not experienced post-collisional stretching on the lithosphere scale: the roots of the crust are preserved in Appalachians, in the Limpopo belt (South Africa), in some areas of the Grenville front, under the Kapuskasing structural zone (of the Superior province) of Canadian Shield (Mareschal, 1994; Percival, 1990).

### Intracontinental collision model

General features of the structure of the thrust zones in areas of continental collision are the presence of rocks of varying degrees of metamorphism, brought to the surface as a result of erosion and uneven uplift, gravitational and magnetic anomalies, often significant thickening of the crust under the thrust zone and in its vicinity, heterogeneity of the velocity field of seismic waves and complex structural constitution. This is due to the fact that the formation and evolution of the Earth's crust in the vicinity of the fault, along which the thrust and uplift of the upper layer takes place, can in principle be described by one process. During a collision, one continental block advances on another; subsequent uplift and erosion lead to the appearance on the surface of rocks up to the lower crust with an increase in the degree of metamorphism in the direction along the fault surface of the overriding block. The study of collision structures is carried out on the basis of a complex model of thermal and dynamic evolution of the thrust region for the rheologically stratified lithosphere and includes a rigid upper crust,

a lower crust and a lithospheric upper mantle divided into blocks, which differ in effective viscosity values. The problem is solved by the finite-element method using a grid deformed in time (Lagrange method). The horizontal reduction of the crust is accompanied by the thrust along the fracture of the blocks of the upper crust along the inclined zone of disturbances, the appearance of additional stress on the layers lying under this zone, and the erosion of the formed overlying rocks. These processes are compensated by viscous flows at the depths of the lower crust and upper mantle (Parphenuk et al., 1994; Parphenuk, Mareschal, 1998). The advantage of the Lagrange method is the ability to calculate real values of strain rates, values of total and shear stresses and, accordingly, deformation of the Moho boundary, fault zone and surface relief during the redistribution of additional load in the region of thrust during the formation of uplifts and their erosion. The software package for calculating the fields of velocities, stresses and temperatures was developed using the elements of the algorithm presented in the monograph (Reddy, 1984). The modeling of viscous flows at the depths of the lower crust and the lithospheric upper mantle within the framework of the equation of motion and continuity was carried out in the Newtonian rheology approximation for a two-layer incompressible viscous fluid. The problem of the distribution of the velocity field and stress is solved by the finite element method:

$$\begin{cases} \mu_i \nabla^2 \mathbf{u} - \nabla P - \rho_i \mathbf{g} = 0 \\ \nabla \mathbf{u} = 0. \end{cases} \quad (1)$$

Here  $P$  is the pressure,  $\mathbf{u}$  is the velocity vector,  $\rho$  is the density,  $\mu$  is the effective kinematic viscosity ( $\mu = \text{const}$ ),  $\mathbf{g}$  is the acceleration of gravity,  $\nabla$  is the linear differential operator,  $\nabla^2 = \nabla \cdot \nabla$  is the Laplace operator.



Based on the solution of the system of equations (1), calculations are made of the thermal evolution of a region that is deformable in the course of a collision, including the upper crust (with the thrust), enriched with radioactive elements. The energy conservation equation for the case of generalized Lagrangian coordinates is formulated as the heat equation without an inertial term, which is contained in the substantial (full) time derivative:

$$c_i \rho_i \frac{DT}{Dt} = \lambda_i \nabla^2 T + H_i, \quad (2)$$

where  $c$  is the specific heat capacity,  $\rho$  is the density,  $\lambda$  is the coefficient of thermal conductivity,  $H$  is the rate of heat generation. The indices correspond to layers with different thermal properties:  $i = 1$  – the lower crust,  $i = 2$  – the upper mantle,  $i = 3$  – the upper crust. It is assumed that the initial state of the crust and lithosphere is defined as a state of thermal equilibrium at constant surface temperature  $T = 0^\circ\text{C}$  and temperature at the base of the lithosphere  $T = 1160^\circ\text{C}$ . The vertical boundaries are thermally insulated (the heat flow is zero). At the boundaries of layers with different thermophysical properties, the temperature continuity condition is satisfied.

The geometry of the study area, along with the main parameters of the problem and the boundary conditions, is presented in Fig. 4. Calculations of thermal evolution were carried out on a deformed mesh obtained in the process of solving the mechanical problem (1) and completed in the region of the upper crust ( $i = 3$ ). The statement of the problem and the boundary conditions are described in detail in (Parphenuk, Mareschal, 1998; Parphenuk, 2015, 2016).

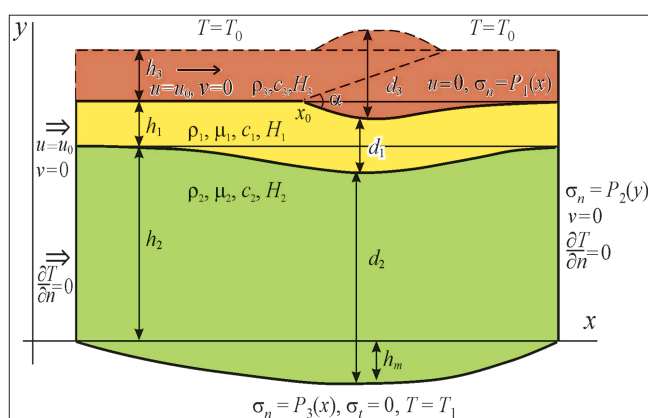


Fig. 4. Geometry of the deformation model for mechanical and thermal problems: the upper crust ( $i = 3$ ) is brown, the lower crust ( $i = 1$ ) is yellow, the lithospheric upper mantle ( $i = 2$ ) is green.  $h_1, h_2, h_3$  are the initial values of the thickness of the lower crust, the upper mantle and the upper crust,  $h_m$  is the deviation of the lower boundary;  $d_1, d_2, d_3$  are the thicknesses of the lower crust, lithospheric mantle and upper crust in the process of deformation,  $u_0$  is the rate of horizontal contraction,  $\alpha$  is the angle of incidence of the fault

### Formation of a collision structure during and after thrusting

The structure of the lithosphere, resulting from the collision thickening of the crust, largely determines the further evolution of the mountain belts that have experienced horizontal compression. As a result of the thrust, the “cold” layer appears under the “hot” layer, and under the effect of an additional load, redistributed during erosion and sedimentation, a gravitationally unstable structure arises. With geologically acceptable strain rates of  $10^{-15}$  to  $10^{-14} \text{ s}^{-1}$  viscous flow at the level of the lower crust and lithospheric upper mantle, the combination of crustal shortening by 70-100 km and additional load during thrust leads to the formation of “roots” of the crust 10-20 km deep 100-200 km. The erosion of the lifted overriding mass brings to the surface plutonic rocks of varying degrees of metamorphism (Parphenuk, 2014). The process of redistributing the load during erosion plays an important role after the end of horizontal compression, preventing the erosion of the formed roots of the crust and the deepening of the upper crust, as it increases the wavelength of the border of the Moho deepening (Parphenuk et al., 1994). The post-collisional stage of evolution is modeled by a change in the boundary conditions after the end of the thrust: in the case of a gravitational instability of the formed structure, the horizontal compression is replaced by stretching and the surface load is redistributed due to ongoing processes of denudation and sedimentation. These processes lead to a reduction of the crustal roots depth (Fig. 5).

The conditions for the formation of crustal roots and the degree of influence of various parameters in the process of advancing plates (the value and contrast of viscosities, the limiting fracture angle, the duration and erosion rate of the uplifts formed) are described in detail in (Parphenuk, 2014; Parphenuk, 2015). In an earlier paper (Parphenuk et al., 1994), estimates were obtained of the possibility of preserving the “roots” of the crust in an environment of gravitational instability of the formed thickening, based on the magnitude of the horizontal extent of the Moho depression. The areas of partial melting, which lead to the formation of collisional granitoids, are largely determined by the geometry and topography of the structures formed in the process of thrust (Jaupart, Provost, 1985).

### Comprehensive analysis of the influence of the thermophysical properties of the Earth's crust on the thermal regime and the dynamics of partial melting zones

In the Earth's crust of recent collisional mountain structures (for example, the Himalayas), there are quasi-steady state melt horizons, marked by geophysical and indirect geological data. They occur at depths of

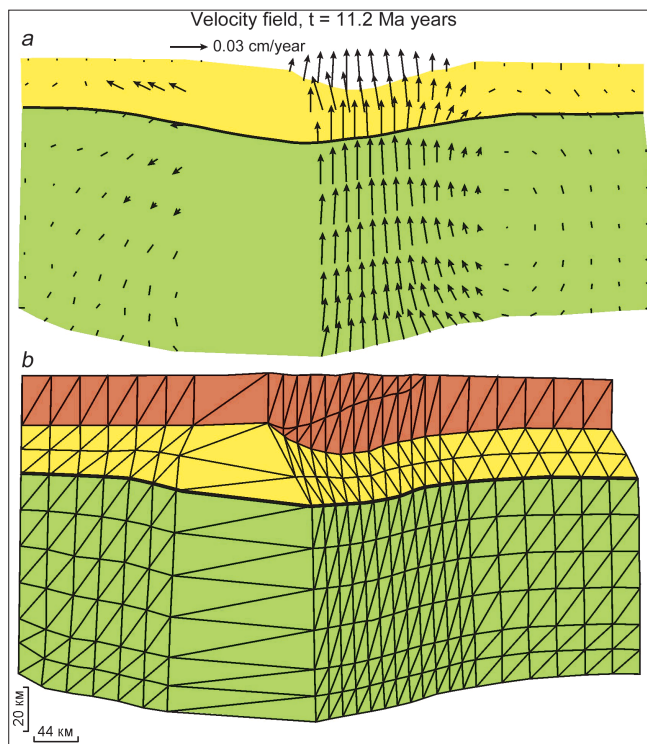


Fig. 5. (a) Distribution of the velocity field of viscous flows in the lower crust and the lithospheric upper mantle at the post-collisional stage (approximately 4 million years after the end of the shortening of 70 km at a rate of 1 cm/year) at an erosion rate of elevated covers of 1 mm/year. The thick line represents the Moho boundary. (b) The geometry of the model, including the upper crust, at the time of completion of the thrust. The effective viscosity is assumed to be  $10^{22}$  Pa·s for the lithospheric upper mantle

10-15 km, have a thickness of about 10 km over a length of 50-250 km, and in physical properties correspond to granite in a state close to the solidus temperature. The possible reason for their appearance is considered to be the melting of the crust substance due to collisional heating during thermal relaxation of the thrust plates (Rosen, Fedorovskii, 2001).

The objective of studying the thermal evolution of collision structures formed by the thrust mechanism is to determine the influence of the values of heat generation and thermal conductivity of the upper crust on the thermal evolution of these areas in connection with the assessment of the possibility of the formation of granite melts. The main source of heating of the continental crust is the heat of decay of long-lived radioactive elements – uranium  $^{235}\text{U}$ ,  $^{238}\text{U}$ , thorium  $^{232}\text{Th}$  and potassium  $^{40}\text{K}$ . The content of these elements is a key parameter for assessing the thermal regime of the continents and the evolution of the mantle substance in the process of crust extraction. Estimates of average concentrations of  $^{235}\text{U}$ ,  $^{238}\text{U}$ ,  $^{232}\text{Th}$  and  $^{40}\text{K}$  differ by almost two times, which leads to average values of the volume heat generation in the range of  $0.55$ - $1.31$   $\mu\text{W}/\text{m}^3$ . The average surface heat generation for various Archean and Proterozoic geological provinces, obtained by systematic sampling over large areas, yields a spread of

values in an even wider range of  $1.01$ - $3.6$   $\mu\text{W}/\text{m}^3$  (Jaupart, Mareschal, 2004, 2011).

A detailed study of the distribution of heat flow density and radioactive crust heat generation in provinces of different ages allowed the authors of the work (Jaupart, Mareschal, 2004) to estimate the total heat generation of the Earth's crust:  $0.56$ - $0.73$   $\mu\text{W}/\text{m}^3$  for the Archean,  $0.73$ - $0.90$   $\mu\text{W}/\text{m}^3$  for the Proterozoic and  $0.95$ - $1.1$   $\mu\text{W}/\text{m}^3$  for the Phanerozoic and Paleozoic with a crust thickness of about 40 km. Taking into account the age of the structures and the fact that the lower crust is depleted of radioactive elements, these estimates in the case of the upper crust should be increased assuming the values of the thickness of the upper crust. The influence of the thermophysical parameters of the thrust structure on its evolution is presented for the scenario of crustal shortening with a rate of  $0.5$  cm/year for 20 million years with erosion and simultaneous sedimentation, which began 5 million years after the onset of thrust. The initial angle of incidence of the fault slipping plane is  $15^\circ$ . The total value of the horizontal shortening is 100 km, the erosion rate is assumed to be  $0.5$  mm/year, decreasing to  $0.25$  mm/year at the post-collision stage. Calculations showed that the velocity of thrusting and erosion have a significant effect on the formation of the surface elevation and a weak influence on the topography of the Moho depression – the main cause of the gravitational instability of the thrust structure (Parphenuk, 2015). For thermal calculations, we used the strain history for the effective viscosity of the thickened lower crust of  $10^{22}$  Pa·s and  $10^{23}$  Pa·s of the upper mantle. The main parameters of the calculations are given in Table 1.

This paper discusses options with heat generation  $1.5$ ;  $2$  and  $2.5$   $\mu\text{W}/\text{m}^3$  in the thickened upper crust (Table 1), which may correspond to the Paleozoic, Proterozoic, and Early Proterozoic settings (when heat generation was  $\sim 1.6$  times higher than presently). Approximately such values of heat generation are taken in a well-known work (England, Thompson, 1984) for a one-dimensional model of instantaneous thrust.

	Upper crust ( $i = 3$ )	Lower crust ( $i = 1$ )	Upper mantle ( $i = 2$ )
Specific heat capacity ( $c$ , J/kg·K)	$10^3$	$10^3$	$10^3$
Thermal conductivity ( $\lambda$ , W/m·K)	1.5; 2.5; 3.0	3	4
Heat generation rate ( $H$ , $\mu\text{W}/\text{m}^3$ )	1.5; 2.0; 2.5	1.1	0.08
Density ( $\rho$ , kg/m $^3$ )	2750	3000	3300
Effective viscosity ( $\mu$ , Pa·s)	-	$10^{22}$	$10^{23}$
Layer thickness ( $h$ , km)	20	20	80

Table 1. The values of the basic parameters for the mechanical and thermal problems of modeling the evolution of the structure of the intracratonic thrusting (Parphenuk, 2016)

It is assumed that the thermal conductivity of the studied layers of the lithosphere does not depend on pressure and temperature. Analysis of the thermal conductivity of the rocks of the Earth's crust shows that the vast majority of definitions fall in the range of 1.5-3.5 W/m·K except for rocks with a high content of quartz, which have higher values of this parameter (Jaupart, Mareschal, 2011). In addition, most silicate materials are characterized by significant anisotropy, and their thermal conductivity depends on the direction. Increased values of thermal conductivity are measured along the stratification of rocks with values of the anisotropy coefficient in the range 1.1-1.5 (Popov et al., 2008; Jaupart, Mareschal, 2011). In our model calculations, we assume that the thermal conductivities of the three layers and 3 different values for  $\lambda$  of the upper crust are constant (Table 1). A model with an increased thermal conductivity of the upper crust in the direction of the main deformation of the horizontal contraction with anisotropy coefficient 1.2 was also calculated.

Let us consider the influence of two main thermal parameters on the redistribution of deep temperatures and its manifestation in the value of the surface heat flow. Fig. 6 shows a picture of the thermal field for the "normal" value of heat generation at different values of the thermal conductivity coefficient 42 million years after the end of the thrusting.

Calculations with different values of heat generation and thermal conductivity of the upper crust showed the possibility of formation a region of partial melt at depths of 30-40 km at different points in time. For a given set of thermophysical parameters, the maximum temperature range is 590-750°C (from the initial 460°C at a depth of 20 km) and 670-885°C (from the initial 610°C at a depth of 30 km) after a horizontal shortening of 100 km over 20 Ma (Parphenuk, 2016). The further rate of temperature increase during the 42 million years of post-collisional evolution is much smaller, which demonstrates the important role of the initial heating phase during the slow thrust and the formation of a thickened crust. Calculations have shown that with the mid-continental initial temperature, most models provide the possibility of the appearance of a partial melt in conditions of "wet" granite. The zone of excess temperature of the solidus of "wet" granite (Perchuk, 1973) occurs at the level of the lower crust, and after the end of contraction and thrust, the upper boundary of the melting region rises to a depth of 15-20 km. The partial melt zone gradually expands and captures the area in front of the thrust front due to the thickening of the crust and the presence of horizontal heat transfer and covers an area of 150-200 km long at the post-collision stage. The temperature increase can be quite significant (up to 320°C) at a depth of 10-30 km.

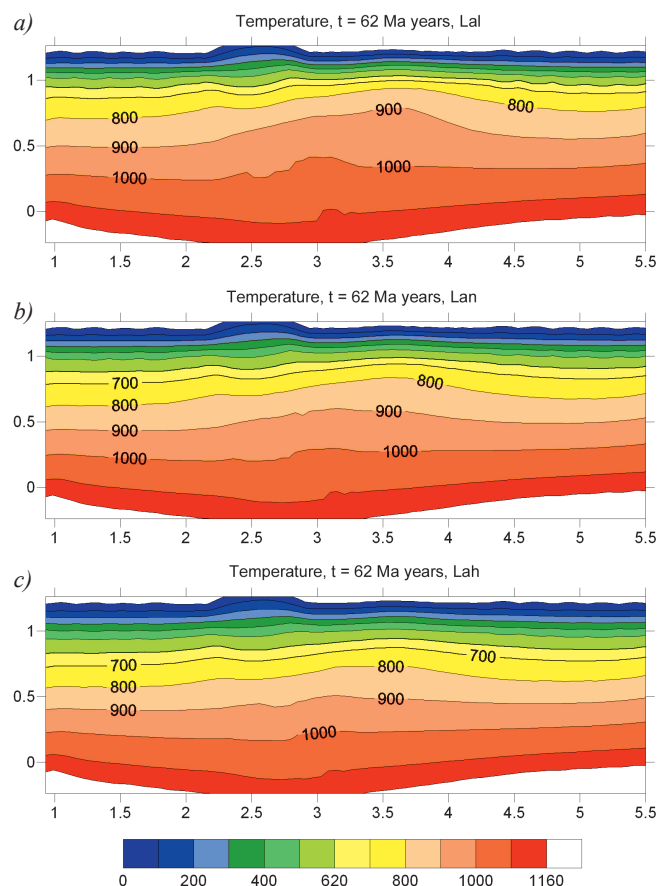


Fig. 6. Temperature distribution for the variant "normal" heat generation rate of  $2.0 \mu\text{W}/\text{m}^3$  ( $H_n$ ) for different values of the thermal conductivity of the upper crust: (a)  $\lambda = 2.0 \text{ W}/\text{m}\cdot\text{K}$  (Lal – low); (b)  $\lambda = 2.5 \text{ W}/\text{m}\cdot\text{K}$  (Lan – normal); (c)  $\lambda = 3.0 \text{ W}/\text{m}\cdot\text{K}$  (Lah – high). Vertical and horizontal scales 1: 100 km

The surface manifestation of the deep processes of temperature redistribution is the heat flow density. The results of modeling the thermal field, reflected in the distribution and evolution of the heat flow, are shown in Fig. 7 and 8. The increase in thermal conductivity (Fig. 7a) or the rate of heat generation (Fig. 7b) leads to almost the same distribution of the heat flow density over the thickened crust at the post-collision stage – 42 Ma after the end of the thrusting.

The broken line in fig. 7a shows the heat flow distribution for the case of anisotropy of thermal conductivity with  $\lambda_x = 1.2 \lambda_y$  for the "normal" set of values of thermal parameters (2). The decrease in the vertical heat flow in this case is quite significant – almost 20% of the maximum values, and it is mainly caused by an increase in the heat transfer in the horizontal direction. As in the case of temperature distribution, the maximum values of heat flow are characteristic of the most thickened section of the upper crust (~ 80 km to the right of point  $x_0$ , Fig. 4 – coordinates of the appearance of an additional load).

Figure 8 presents the results of calculations of the evolution of heat flow over the region of the maximum perturbed thermal field (~ 80 km to the right of point  $x_0$



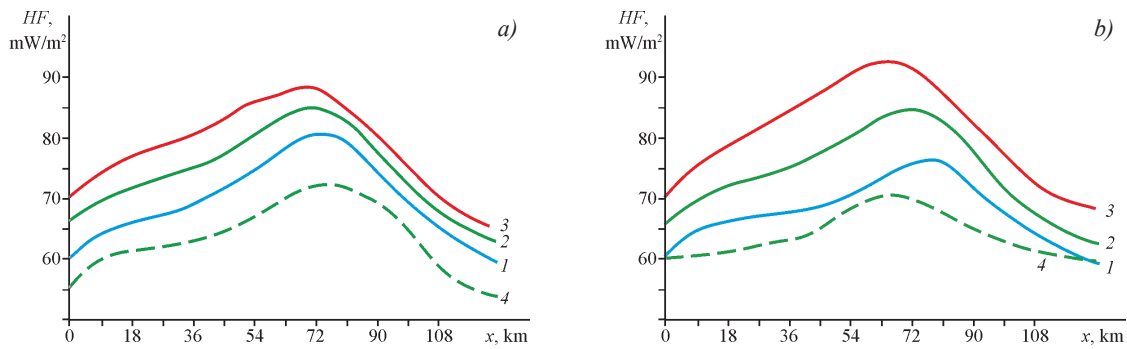


Fig. 7. The distribution of the heat flow density over the uplift (point 0 in the horizontal direction corresponds to the point  $x_0$  in Fig. 4) 42 million years after the end of the horizontal contraction process. (a) Effect of thermal conductivity  $\lambda$ : 1 – 2.0 (low), 2 – 2.5 (normal), 3 – 3.0 (high) W/m·K. The discontinuous curve (4) represents the result for the case of thermal conductivity anisotropy  $\lambda_x = 1.2 \lambda_y$ , (b) Influence of the rate of heat generation of the upper crust  $H$ : 1 – 1.5 (low), 2 – 2.0 (normal), 3 – 2.5 (high)  $\mu\text{W}/\text{m}^3$ . The discontinuous curve (4) represents the distribution of the heat flow at the time of the end of the thrusting ( $t \sim 20$  Ma) for the “normal” model (2)

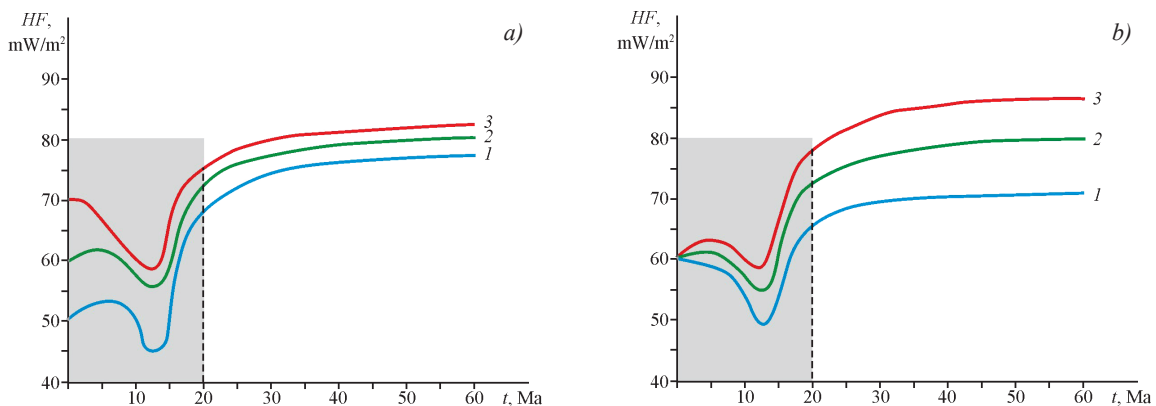


Fig. 8. Evolution of heat flow from the surface above the area of maximum uplift. (a) Options with different values of thermal conductivity  $\lambda$ : 1 – 2.0 (low), 2 – 2.5 (normal), 3 – 3.0 (high) W/m·K with an average value of heat generation  $2.0 \mu\text{W}/\text{m}^3$ . (b) Influence of various rates of heat generation  $H$ : 1 – 1.5 (low), 2 – 2.0 (normal), 3 – 2.5 (high)  $\mu\text{W}/\text{m}^3$  with an average value of thermal conductivity  $2.5 \text{ W}/\text{m}\cdot\text{K}$ . Shaded area – the period of thrusting

in Fig. 4) for different values of thermal conductivity  $\lambda$  (a) and heat generation rate  $H$  (b).

According to the simulation results, the heat flow density drops by about  $10 \text{ mW}/\text{m}^2$  over the limiting fault during the thrusting (shaded area in the figure). The physical basis of this phenomenon is that a layer of a certain thickness (in our model, this is the upper crust) with the same initial temperature distribution gradually moves on a plate with some initial temperature distribution. As a result of the thrust, the “cold” layer is under the “hot” layer and then the temperature equalization stage follows. The early postcollisional stage is characterized by a slight increase in heat flow due to an increase in the thickness of the upper crust with maximum heat generation. Further, the heat flow reaches stable values, since the redistribution of additional load caused by erosion of uplift and sedimentation is very insignificant at this stage due to the local nature of erosion assumed in the model.

**Discussion of the results and conclusions**

Table 2 presents a sample of temperatures for all 9 models with three different values of heat generation

$\frac{460}{610}$	$H_l = 1.5$ $\mu\text{W}/\text{m}^3$	$H_n = 2.0$ $\mu\text{W}/\text{m}^3$	$H_h = 2.5$ $\mu\text{W}/\text{m}^3$
$\lambda_l = 2.0 \text{ W}/\text{m}\cdot\text{K}$	<u>685</u> 730	<u>780</u> 840	<u>715</u> 755
$\lambda_n = 2.5 \text{ W}/\text{m}\cdot\text{K}$	<u>630</u> 700	<u>700</u> 770	<u>665</u> 720
$\lambda_h = 3.0 \text{ W}/\text{m}\cdot\text{K}$	<u>590</u> 670	<u>615</u> 705	<u>620</u> 690

Tab. 2. The temperature values ( $^{\circ}\text{C}$ ) under the midpoint of the uplift at the end of the thrusting ( $t = 19.4$  Ma) are left columns and in the post-collisional stage ( $t = 62$  million years) – right columns. The first cell shows the initial temperatures of the selected depths of 20 and 30 km, respectively. Details are given in the text

of the upper crust ( $H_l, H_n, H_h$ ) – horizontally, and three values of thermal conductivity ( $\lambda_l, \lambda_n, \lambda_h$ ) – vertically. It shows temperatures at the end of the thrusting  $\sim 20$  million years (left columns in all columns) and 42 million years after the end of the thrusting ( $t = 62$  million years – right columns). The upper values are for a depth of  $\sim 20$  km (the boundary of the upper and lower crust), the lower values for a depth of  $\sim 30$  km (lower crust) below the midpoint (maximum) elevation point,

at a distance of about 80 km to the right of the point  $x_0$  (Fig. 4). Calculations have shown that this is the region of maximum temperatures in the horizontal direction due to the maximum thickening of the crust with high heat generation. The expected result is the maximum temperature increase at the post-collision stage in the case of maximum generation and minimum thermal conductivity ( $H_h$  and  $\lambda_c$ ). The average temperature increase after the end of the thrusting is approximately 200°C for the upper crust (the initial temperature of the model is 460°C for the boundary of the upper and lower crust at a depth of 20 km) and 110°C for a depth of 30 km (in the lower crust). In most variants of thermophysical parameters, the temperature at the final stage of thrusting and at the post-collision stage, with the exception of a high value of thermal conductivity, exceeds the solidus temperature of “wet” granite (shown in bold in Table 2). These results under conditions of local erosion confirm the main conclusions of a one-dimensional simulation of instantaneous thrust about the possibility of the formation of partial melting zones under certain thermal conditions (England, Thompson, 1984).

For the set of selected thermophysical parameters, the calculated maximum temperature range is 590–750°C (from the initial 460°C) and 670–885°C (from the initial 610°C) after a horizontal reduction of 100 km with a thrusting duration of 20 Ma. In the future, the temperature increase rate for 42 million years of post-collisional evolution is much less (compared with the columns on the right), which demonstrates the important role of the initial heating phase during the slow thrusting and the formation of a thickened crust. Thus, with the mid-continental initial temperature, most models provide the possibility of the appearance of a partial melt in the solidus conditions of “wet” granite (the temperatures indicated in bold in Table 2).

The evolution of heat losses at the stage of motion during thrusting and after its termination is studied. The density of the heat flow drops by about 10 mW/m<sup>2</sup> over the fault, along which the process of thrusting occurs. The early postcollisional stage is characterized by a slight increase in heat flow due to an increase of the upper crust thickness, in which heat generation is maximum. Further, the heat flow reaches stable values, since the redistribution of additional load caused by erosion of uplift and sedimentation is very insignificant at this stage due to the local nature of erosion assumed in the model. The maximum values of the heat flow density in the frontal thrust area at the post-collisional stage are 85–95 mW/m<sup>2</sup> with regional background values of 50–70 mW/m<sup>2</sup>. It has been shown that heat losses from the surface after the end of the crust shortening are more dependent on the values of heat generation than on the thermal conductivity of the upper crust.

## Acknowledgements

This work was supported by the State budget theme No. 0144-2014-0086.

## References

- Barbey P., Convert J., Moreau B. et al. (1984). Petrogenesis and evolution of an Early Proterozoic collisional orogen: the Granulite Belt of Lapland and the Belomorides (Fennoscandia). *Bull. Geol. Soc. Finl.*, 56, pp. 161–188. <https://doi.org/10.17741/bgsf/56.1-2.010>
- England P., Thompson A.B. (1984). Pressure – temperature – time paths of regional metamorphism. Part I: Heat transfer during the evolution of regions of thickened continental crust. *J. Petrology*, 25, pp. 894–928. <https://doi.org/10.1093/petrology/25.4.894>
- Gaal G., Berthelsen A., Gorbatshev R. et al. (1989). Structure and composition of the Precambrian crust along the POLAR Profile in the northern Baltic Shield. *Tectonophysics*, 162, pp. 1–25. [https://doi.org/10.1016/0040-1951\(89\)90354-5](https://doi.org/10.1016/0040-1951(89)90354-5)
- Gerdes A., Worner G., Henk A. (2000). Post-collisional granite generation and HT – LP metamorphism by radiogenic heating: the Variscan South Bohemian Batholith. *Journal of the Geological Society*, 157, pp. 577–587. <https://doi.org/10.1144/jgs.157.3.577>
- Jaupart C., Mareschal J.-C. (2004). Constraints on crustal heat production from heat flow data. *Treatise on Geochemistry*, V. 3: The Crust. Ed. by R.L. Rudnick. Amsterdam: Elsevier Sci. Pub., pp. 65–84.
- Jaupart C., Mareschal J.-C. (2011). Heat generation and transport in the Earth. New York: Cambridge Univ. Press, 464 p.
- Jaupart C., A. Provost (1985). Heat focusing, granite genesis and inverted metamorphic gradients in continental collision zones. *Earth Planet. Sci. Lett.*, 73, p. 385–397. [https://doi.org/10.1016/0012-821X\(85\)90086-X](https://doi.org/10.1016/0012-821X(85)90086-X)
- Luosto U., Flueh E.H., Lund C.-E. (1989). The crustal structure along the POLAR Profile from seismic refraction investigations. *Tectonophysics*, 162, pp. 51–85. [https://doi.org/10.1016/0040-1951\(89\)90356-9](https://doi.org/10.1016/0040-1951(89)90356-9)
- Mareschal J.-C. (1994). Thermal regime and post-orogenic extension in collision belts. *Tectonophysics*, 238, pp. 471–484. [https://doi.org/10.1016/0040-1951\(94\)90069-8](https://doi.org/10.1016/0040-1951(94)90069-8)
- Parphenuk O.I. (2014). Analiz vliyaniya erozii kollizionnykh podnyatii na protsess ekskumatsii glubinnykh porod (chislennoe modelirovanie) [Analysis of the collisional uplifts erosion influence on the overthrust structures and the process of deep crustal rocks exhumation (numerical modeling)]. *Vestnik KRAUNTs = Bulletin of Kamchatka Regional Association «Educational-Scientific Center»*. *Earth Sciences*, 1(23), pp. 107–20. (In Russ.)
- Parphenuk O.I., Mareschal J.-C. (1998). Numerical modeling of the thermomechanical evolution of the Kapuskasing structural zone, Superior province, Canadian shield. *Izvestiya. Physics of the Solid Earth*, 10, pp. 22–32. (In Russ.)
- Parphenuk O.I. (2015). Uplifts formation features in continental collision structures (evolution modeling). *Russian Journal of Earth Sciences*, 15, ES4002, 8 p. <https://doi.org/10.2205/2015ES000556>
- Parphenuk O.I. (2016). Thermal regime and heat transfer during the evolution of continental collision structures. *Russian Journal of Earth Sciences*, 16, ES6006, 10 p. <https://doi.org/10.2205/2016ES000589>
- Parphenuk O.I., Dechoux V., Mareschal J.-C. (1994). Finite-element models of evolution for the Kapuskasing structural zone. *Can. J. Earth Sci.*, 31(7), pp. 1227–1234. <https://doi.org/10.1139/e94-108>
- Perchuk L.L. (1973). Termodinamicheskii rezhim glubinogo petrogeneza [Thermodynamic regime of deep petrogenesis]. Moscow: Nauka, 318 p. (In Russ.)
- Perchuk L.L., Krotov A.V., Gerya T.V. (1999). Petrologiya amfibolitov poyasa Tana i granulitov Laplandskogo kompleksa [Petrology of amphibolites of the Tana belt and granulites of the Lapland complex]. *Petrologiya = Petrology*, 7(4), pp. 356–381. (In Russ.)
- Percival J.A. (1990). A field guide through the Kapuskasing uplift, a cross section through the Archean Superior Province. *Exposed Cross-Sections of the Continental Crust*, NATO ASI Ser., 317, pp. 227–283. [https://doi.org/10.1007/978-94-009-0675-4\\_10](https://doi.org/10.1007/978-94-009-0675-4_10)
- Popov Yu.A., Romushkevich R.A., Miklashevskii D.E. et al. (2008). Novye rezul'taty geotermicheskikh i petroplevnykh issledovaniy razrezov kontinental'nykh nauchnykh skvazhin [New results of geothermal and petrothermal studies of the sections in continental scientific wells]. *Teplivoe pole Zemli i metody ego izucheniya* [Proc. Int. Conf. «The Earth's Thermal Field and Related Research Methods»]. Ed. Yu.A. Popov. Moscow: RIO RGGRU, pp. 208–212. (In Russ.)
- Reddy J.N. (1984). An introduction to the Finite Element Method. McGraw-Hill: New-York, 459 p.



Rozen O.M., Fedorovskii V.S. (2001). Kollizionnye granitoidy i rassloenie zemnoi kory [Collisional granitoids and stratification of the Earth's crust]. *Trudy GIN RAN* [Proceedings of Geological Institute of RAS], 545, 188 p. (In Russ.)

Sharov N.V. (1993). Litosfera Baltiiskogo shchita po seismicheskim dannym [Lithosphere of the Baltic Shield according to seismic data]. Apatity: KNTs RAN, 145 p. (In Russ.)

Sokolov S.D. (1990). Kontsepsiya tektonicheskoi rassloennosti litosfery: istoriya sozdaniya i osnovnye polozheniya [The concept of tectonic stratification of the lithosphere: the history of foundation and the main aspects]. *Geotektonika = Geotectonics*, 6, pp. 3-19. (In Russ.)

*Tectonophysics*. (1989). Special Issue: The European Geotraverse, Part 5: The Polar Profile. 162(1-2), 171 p.

## About the Author

*Olga I. Parphenuk* – DSc (Physics and Mathematics),  
Leading Researcher, Laboratory of the Theoretical  
Geophysics

Schmidt Institute of Physics of the Earth of the  
Russian Academy of Sciences

Buil. 1, 10, B. Gruzinskaya st., Moscow, 123242,  
Russian Federation

Phone: +7 (499) 254 23 18, e-mail: [oparfenuk@ifz.ru](mailto:oparfenuk@ifz.ru)

*Manuscript received 19 July 2018;*

*Accepted 20 September 2018;*

*Published 30 November 2018*

